ALKALINE HYDROGEN EVOLUTION ON CO-M@gCN DUAL-ATOM CATALYSTS: INSIGHTS FROM FIRST-PRINCIPLES CALCULATIONS

PHẢN ỨNG TIẾN HÓA HYDRO TRONG MÔI TRƯỜNG KIỀM TRÊN CHẤT XÚC TÁC HAI NGUYÊN TỬ CO-M@gCN: PHÂN TÍCH TỪ TÍNH TOÁN NGUYÊN LÝ THỨ NHẤT

Tran Thi Kim Cuc[1,2], Thuy T. T. Duong[1,3], Ho Van Binh[4], Tien B. Tran[5], Thi H. Ho[6,7], Bich-Tram Truong Le[5], Dang Kim Hoang[1], Viet Q. Bui[1]*

[1]*Advanced Institute of Science and Technology, The University of Danang, Danang, Vietnam*
[2]*Master student at Department of Chemistry, University of Sciences, Hue University, Vietnam*
[3]*Master student at Department of Chemistry, University of Science – VNUHCM, Vietnam*
[4]*University of Science – VNUHCM, Vietnam*
[5]*The University of Danang, Vietnam*
[6]*Institute for Computational Science and Artificial Intelligence, Van Lang University, Ho Chi Minh City, Vietnam*
[7]*Van Lang University, Ho Chi Minh City, Vietnam*

*Corresponding author: mrbuiquocviet@gmail.com; bqviet@ac.udn.vn

(Received: May 13, 2025; Revised: June 30, 2025; Accepted: July 05, 2025)

DOI: 10.31130/ud-jst.2025.23(7).320E

Abstract - Dual-atom catalysts (DACs) offer unique opportunities for enhancing electrocatalytic performance through synergistic metal interactions. Herein, we employ spin-polarized density functional theory to investigate Co-M DACs (M = Cr, Mn, Fe, Co, Ni, Cu, Pd, Ru, Ir, Pt) supported on graphitic carbon nitride (gCN) for the hydrogen evolution reaction (HER) in alkaline media. Among the examined systems, CoCr@gCN demonstrates the best performance with a low water dissociation barrier (0.42 eV), nearly thermoneutral hydrogen adsorption ($\Delta G_{H^*} \approx 0.03$ eV), and half-metallic behavior. Electronic descriptors such as iCOHP, Bader charge, and a φ parameter based on metal properties help elucidate activity trends. Systems with φ in the range of 4.5-4.6 exhibit enhanced catalytic properties. Ab initio molecular dynamics simulations confirm the thermal stability of CoCr@gCN at 400 K. This work provides insights into the design of efficient and earth-abundant DACs for sustainable hydrogen production.

Keywords - Dual-atom catalysts; Hydrogen evolution reaction; Density functional theory; Graphitic carbon nitride; Descriptor analysis.

Tóm tắt - Chất xúc tác hai nguyên tử kim loại (DACs) mang lại khả năng tăng cường hiệu suất điện hóa thông qua tương tác cộng hưởng giữa các kim loại. Trong nghiên cứu này, chúng tôi sử dụng lý thuyết phiếm hàm mật độ có xét spin để khảo sát các hệ Co-M@gCN (M = Cr, Mn, Fe, Co, Ni, Cu, Pd, Ru, Ir, Pt) trong phản ứng tiến hóa hydro (HER) ở môi trường kiềm. Hệ CoCr@gCN cho hiệu suất cao nhất với hàng rào phân tách nước thấp (0,42 eV), hấp phụ H* gần trung tính ($\Delta G_{H^*} \approx 0,03$ eV), và đặc tính bán kim loại. Các chỉ số như iCOHP, điện tích Bader và thông số φ giúp giải thích xu hướng hoạt tính. Khoảng φ từ 4,5–4,6 tương ứng với hiệu suất tối ưu. Mô phỏng AIMD xác nhận tính ổn định nhiệt động của CoCr@gCN ở 400 K. Công trình này cung cấp những hiểu biết sâu sắc về việc thiết kế các chất xúc tác hai nguyên tử (DACs) hiệu quả và phong phú trong tự nhiên nhằm phục vụ cho quá trình sản xuất hydro bền vững.

Từ khóa - Chất xúc tác hai nguyên tử kim loại; Phản ứng tiến hóa hydro; Lý thuyết phiếm hàm mật độ; Carbon nitride dạng graphitic; Phân tích descriptor điện tử.

1. Introduction

The global demand for sustainable and clean energy technologies has renewed significant interest in hydrogen as a viable energy carrier. This is due to its high gravimetric energy density and its potential to serve as a carbon-free fuel when generated through water electrolysis [1]. Within this process, the hydrogen evolution reaction (HER) plays a central role in converting electrical energy into chemical energy. However, the efficiency of HER is fundamentally limited by the catalytic performance of the electrode materials. The HER in alkaline media proceeds through a distinct mechanism compared to acidic conditions, where water molecules act as the primary proton source. The reaction typically involves two elementary steps: the Volmer step, which entails water dissociation into adsorbed hydrogen (H*) and hydroxide (OH*), and either the Heyrovsky or Tafel step for hydrogen evolution. This distinction emphasizes the critical role of water activation and OH* desorption in determining catalytic efficiency under alkaline conditions. Although Pt remains the benchmark HER catalyst because of its near-zero overpotential and ideal hydrogen binding energy, its high cost and scarcity severely hinder its application in large-scale hydrogen production [2], [3].

To overcome these limitations, efforts have been directed toward developing alternative catalysts composed of earth-abundant elements. Single-atom catalysts (SACs) have emerged as a promising class of materials due to their maximized atom utilization and well-defined coordination environments, which enhance catalytic selectivity and efficiency [4] - [7]. In typical SAC systems, isolated metal atoms are anchored to nitrogen-containing carbon supports, enabling strong metal-support interactions that stabilize active sites. Despite their advantages, SACs often suffer from a low density of accessible active centers and limited capacity to modulate their local electronic

structure. These shortcomings restrict their ability to facilitate complex multi-step reactions such as the hydrogen evolution reaction [8], [9].

To address these challenges, dual-atom catalysts (DACs) have been introduced as an advanced alternative to SACs. DACs consist of two spatially adjacent yet isolated metal atoms, which allows for synergistic interactions between the metal centers. This configuration enables enhanced modulation of the electronic structure and improved adsorption properties for key intermediates in electrocatalytic reactions [10] - [12]. The deliberate pairing of different metal atoms can create local charge polarization and tune the density of states near the Fermi level, which in turn enhances substrate binding and reaction kinetics [13] - [15].

Graphitic carbon nitride (gCN) has attracted increasing attention as a highly suitable support for DACs. The material possesses a nitrogen-rich framework with well-defined coordination sites, excellent chemical and thermal stability, and low synthetic cost [16] - [18]. Recent density functional theory (DFT) investigations have confirmed the potential of gCN to stabilize various DAC configurations across a broad range of pH environments. Notably, a systematic DFT screening of 55 Co-M@gCN systems identified structures such as CrCo@gCN, FeRu@gCN, and FeIr@gCN as particularly promising for HER. These systems exhibit low kinetic barriers for water dissociation and near-thermoneutral Gibbs free energy changes for hydrogen adsorption, which are key indicators of high catalytic efficiency [18]. Other studies have shown that Ni-Co DACs on gCN outperform their single-atom counterparts in terms of HER activity. This enhancement arises from the cooperative interactions between the two metal atoms, which modulate the adsorption energies of intermediates and facilitate reaction kinetics [19].

In addition, gCN-based supports can be further optimized through heteroatom doping. Incorporating elements such as phosphorus or sulfur has been shown to improve the electronic conductivity and charge transport properties of gCN. These modifications lead to enhanced HER performance and expand the tunability of gCN as a functional support for dual-atom catalysts [20], [21]. Altogether, these findings demonstrate the significant potential of DACs on gCN as next-generation electrocatalysts for efficient and sustainable hydrogen production.

In this study, we employ spin-polarized DFT calculations to systematically investigate a series of Co-M dual-atom catalysts, where M represents transition metals from the 3d (Cr, Mn, Fe, Co, Ni, Cu), 4d (Pd, Ru), and 5d (Pt, Ir) series. These DACs are anchored on gCN, a nitrogen-rich, low-cost, and structurally robust support that provides abundant anchoring sites for stabilizing metal atoms. We examine the thermodynamic stability, electronic structure, and catalytic activity of these Co-M@gCN systems toward HER by calculating both the kinetic barrier for water dissociation and the Gibbs free energy change (ΔG_{H^*}) for hydrogen adsorption. Our results highlight CoCr@gCN as a particularly promising catalyst, exhibiting a low kinetic barrier of 0.42 eV for water dissociation and a nearly thermoneutral hydrogen adsorption energy ($\Delta G_{H^*} \approx 0.03$ eV). These favorable energetic parameters indicate excellent HER performance in both kinetic and thermodynamic aspects. Electronic structure analysis reveals that the enhanced activity arises from optimized electronic interactions between the dual-metal sites and the gCN substrate, which modulate the density of states near the Fermi level and strengthen the binding with key intermediates.

2. Computational methods

All spin-polarized density functional theory (DFT) calculations were performed using the Vienna Ab initio Simulation Package (VASP). The interaction between core and valence electrons was described by the projector-augmented wave (PAW) method, and the exchange-correlation effects were treated using the generalized gradient approximation (GGA) in the Perdew-Burke-Ernzerhof (PBE) functional form. A plane-wave kinetic energy cutoff of 450 eV was employed in all calculations.

The dual-atom catalyst models were constructed by anchoring heteronuclear metal dimers composed of cobalt and another transition metal M (M = Cr, Mn, Fe, Co, Ni, Cu, Pd, Ru, Pt, Ir) on a 2×2 supercell of graphitic carbon nitride (gCN), which contains 50 atoms. The initial positions of the metal atoms were placed on adjacent nitrogen-coordinated sites, followed by full geometry relaxation. A vacuum layer of 20 Å along the z-direction was applied to eliminate periodic image interactions. The Brillouin zone was sampled using a 5×5×1 Monkhorst-Pack k-point mesh for structure optimization, while a denser 7×7×1 grid was used for electronic structure calculations. The total energies were converged to 10^{-5} eV, and the atomic forces were relaxed to below 0.01 eV/Å. The Grimme DFT-D2 method was employed to account for van der Waals interactions. Zero-point energy (ZPE) corrections and entropy contributions at 298.15 K were included for thermodynamic analysis. To evaluate the HER activity, we calculated the Gibbs free energy change (ΔG_{H^*}) of hydrogen adsorption using the computational hydrogen electrode (CHE) model:

$$\Delta G_{ads^*} = \Delta E_{ads^*} + \Delta E_{ZPE} - T\Delta S$$

where, ΔE_{H^*} is the adsorption energy of H*, ΔE_{ZPE} is the zero-point energy difference between the adsorbed H* and gas-phase H_2, and ΔS is the entropy difference at room temperature.

The water dissociation step ($H_2O^* \rightarrow OH^* + H^*$) was investigated under alkaline conditions using the climbing-image nudged elastic band (CI-NEB) method. Five intermediate images were used to connect the initial and final states, allowing identification of the transition state and calculation of the activation energy (E_a). To assess catalyst stability, we computed the binding energy (E_b), and average formation energy (E_f), as follows:

$$E_b = 1/2(E_{CoM@gCN} - E_{gCN} - E_{Co} - E_M) \quad (1)$$

$$E_f = 1/2(E_{CoM@gCN} - E_{gCN} - E_{Co,bulk} - E_{M,bulk}) \quad (2)$$

Finally, Bader charge analysis was performed to

examine charge redistribution between the metal atoms and the gCN substrate, providing insights into the electronic interactions responsible for catalytic activity.

3. Results and discussions

To systematically evaluate the electrocatalytic performance of Co-M dual-atom catalysts anchored on gCN, we first investigated the thermodynamic stability and structural characteristics of each system. The binding energy (E_b) and average formation energy (E_f) were calculated to assess the feasibility of anchoring Co and M atoms (M = Cr, Mn, Fe, Co, Ni, Cu, Pd, Ru, Ir, Pt) on the gCN substrate. Furthermore, geometric parameters such as bond lengths and local atomic environments were examined to understand the role of metal-metal interactions and substrate coordination in determining catalyst stability. The trends in E_b and E_f are then correlated with atomic radius mismatch to provide physical insights into the structural preferences of Co-M@gCN configurations.

3.1. Structural stability of Co-M@gCN catalysts

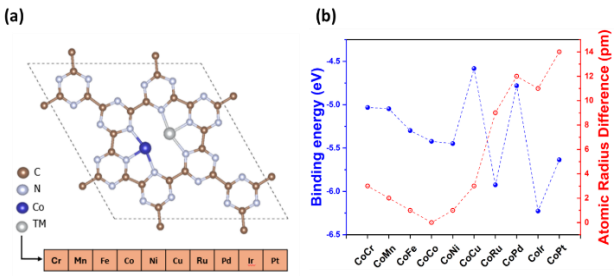

Figure 1. *(a) Schematic illustration of a Co-M dual-atom catalyst anchored on gCN monolayer. Cobalt (Co) and a transition metal (TM) atom are coordinated to nitrogen-rich sites in the gCN framework. (b) Calculated binding energies (blue, left axis) of Co-M@gCN systems and the atomic radius differences (red, right axis) between Co and M atoms, showing their correlation with thermodynamic stability*

Figure 1a illustrates the representative atomic structure of a Co-M dual-atom catalyst anchored on gCN, where two metal atoms (Co and M) are stabilized at adjacent nitrogen-coordinated vacancies. The selected metals span across 3d, 4d, and 5d transition metal series, providing a broad spectrum of electronic environments and atomic radii for systematic evaluation. The corresponding E_b and E_f of all systems are summarized in Table 1 and visually correlated with atomic radius mismatch in Figure 1b. All Co–M@gCN systems exhibit negative E_b values, confirming the thermodynamic stability of dual-metal anchoring on gCN. Among the investigated configurations, CoIr@gCN shows the most negative E_b value of –6.23 eV, indicating the strongest interaction with the substrate. This strong binding may be attributed to the high electronegativity and orbital overlap of Ir with the nitrogen framework of gCN. However, the corresponding E_f value for CoIr@gCN is slightly positive, suggesting that although the anchored structure is energetically stable, its formation from bulk metallic precursors is not thermodynamically favored. A similar observation is made for CoRu@gCN, which also exhibits a positive formation energy despite strong binding. This discrepancy highlights the distinction between binding affinity and formation feasibility, both of which must be considered in evaluating the practical stability of DAC systems.

In contrast, CoMn@gCN exhibits the most negative formation energy (–0.83 eV), indicating that it is the most favorable system to form from the gas-phase precursors. Interestingly, the atomic radius difference between Co and Mn is not the smallest among the examined systems. For instance, CoCo@gCN, by definition, exhibits no atomic radius mismatch, and CoFe@gCN also has a smaller mismatch than CoMn@gCN. These comparisons suggest that structural stability cannot be explained by atomic size compatibility alone. Instead, favorable electronic interactions, including local charge distribution and bonding symmetry, also play essential roles in stabilizing dual-metal configurations.

Table 1. *Calculated binding energies (E_b) and formation energies (E_f) of Co-M@gCN. Negative values of Eb and Ef indicate thermodynamic favorability in metal anchoring and system formation*

Struct.	CoCr	CoMn	CoFe	CoCo	CoNi	CoCu	CoRu	CoPd	CoIr	CoPt
E_b (eV)	-5.03	-5.05	-5.30	-5.42	-5.45	-4.58	-5.92	-4.78	-6.23	-5.63
E_f (eV)	-0.38	-0.83	-0.28	-0.14	-0.35	-0.21	0.20	-0.28	0.09	-0.29

The correlation between E_b and atomic radius difference is more pronounced among the 3d transition metals. As the mismatch increases, such as in the case of CoCu@gCN, the binding energy becomes less negative. This trend is consistent with the expectation that increasing lattice strain and reduced orbital overlap weaken the interaction with the support. However, this relationship becomes less clear when extended to the 4d and 5d series. A case in point is CoPt@gCN, which maintains a relatively strong binding energy despite having the largest atomic radius mismatch. This deviation may be related to extended d-orbital character and relativistic effects in heavier elements, which can compensate for geometric strain. These findings indicate that while atomic radius difference provides a useful metric for predicting structural stability within a given transition metal group, it is insufficient when comparing across periods. A comprehensive evaluation of both geometric compatibility and electronic interactions is required to rationally design stable dual-atom catalysts on gCN supports.

3.2. Electronic structure

To understand the origin of HER activity across different Co-M@gCN systems, we analyzed the projected local density of states (LDOS) for both spin channels, as shown in Figure 2. Several active systems, including CoCr@gCN, CoMn@gCN, CoNi@gCN, and CoRu@gCN, exhibit pronounced half-metallic behavior, characterized by a spin-asymmetric electronic structure: one spin channel remains metallic, offering a continuous density of states at the Fermi level (E_F), while the other shows a finite bandgap.

This spin polarization implies the presence of a spin-selective conduction pathway, which can facilitate electron transfer and modulate the adsorption strength of key HER

intermediates. In particular, CoCr@gCN exhibits a metallic spin-down channel and a narrow ~0.2 eV bandgap in the spin-up channel, a combination that is often associated with efficient charge mobility and favorable intermediate binding energies. Other systems, such as CoFe@gCN and CoPt@gCN, despite being thermodynamically stable, display more symmetric and deeply buried d-states in both spin channels. This can lead to diminished electronic reactivity, as the lower density of available states near E_F limits their ability to form optimal interactions with H_2O*, H*, or OH* species.

These observations suggest that half-metallicity combined with a moderate density of states near E_F in the active spin channel is a key electronic feature correlating with superior HER performance. The presence of spin-polarized conducting states may not only enhance HER kinetics but also offer new possibilities for spin-dependent catalytic mechanisms in dual-atom catalysts.

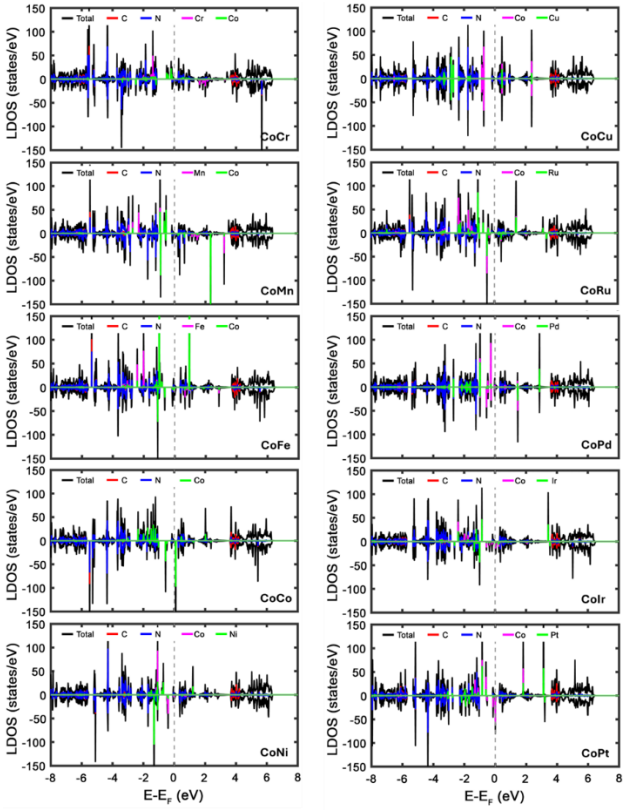

Figure 2. *Projected local density of states (LDOS) of Co-M@gCN systems. Contributions from C, N, Co, and the secondary metal (M = Cr, Mn, Fe, Co, Ni, Cu, Ru, Pd, Ir, Pt) are shown*

3.3. Reaction pathway energetics and mechanism

To elucidate the reaction mechanism of hydrogen evolution on Co-M@gCN catalysts under alkaline conditions, we evaluated two possible pathways involving adsorbed water: one in which OH* desorbs prior to H_2 formation (mechanism i), and another in which molecular hydrogen evolves first while OH* remains temporarily bound (mechanism ii). The computed Gibbs free energy profiles clearly indicate that mechanism (ii), which proceeds via the Volmer-Heyrovsky route ($H_2O^* \rightarrow H^* + OH^* \rightarrow \frac{1}{2} H_2 + OH^*$), is energetically preferred across the majority of systems investigated.

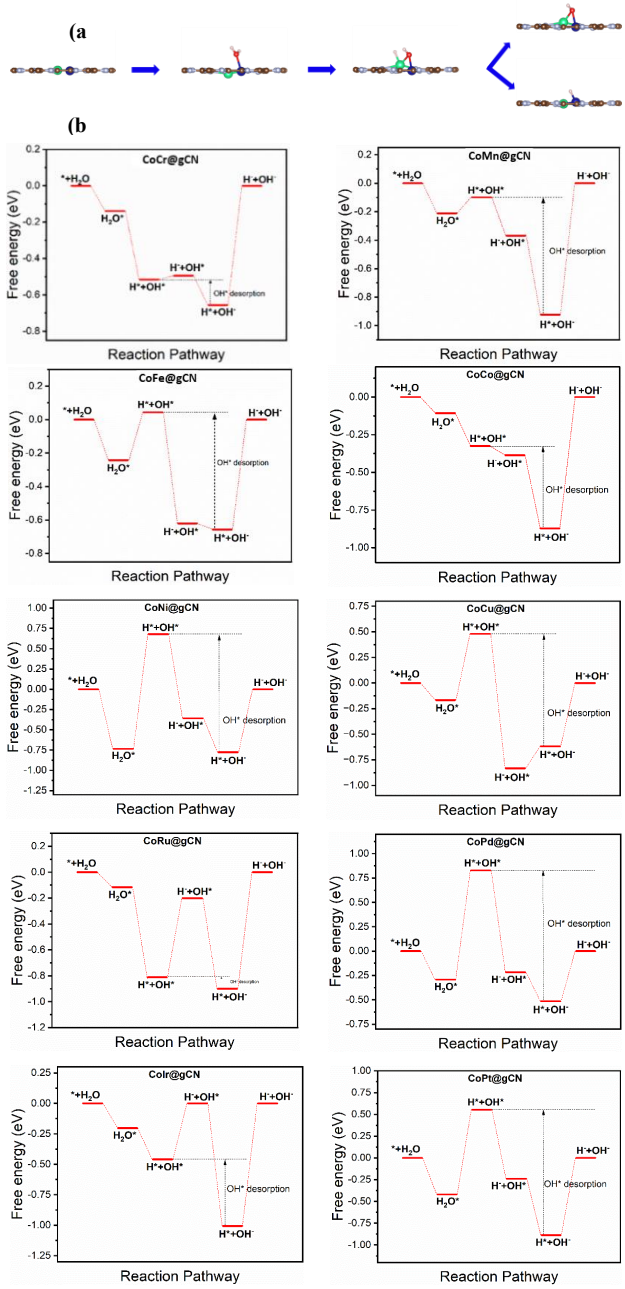

Figure 3. *(a) Reaction pathway of alkaline HER on CoM@gCN, illustrating the H2O activation, H* formation, and subsequent OH* desorption. (b) Free energy profiles of HER via the Volmer-Heyrovsky mechanism for all Co-M@gCN systems*

In this mechanism, the initial step of water dissociation yields surface-bound H* and OH*, followed by a downhill transition leading to hydrogen gas evolution. This pathway not only bypasses the necessity for a second proton-electron pair, but also minimizes the energy penalty associated with strong OH* binding. The critical step governing the overall kinetics is the desorption of OH*, which often presents the highest free energy barrier in the reaction profile. This barrier reflects the delicate balance between ensuring sufficient stabilization of reaction intermediates and facilitating their eventual removal to regenerate the active site. The structural identity of these intermediates was validated through full geometry optimizations after water

dissociation. The relaxed configurations confirm stable adsorption of H* and OH* on adjacent metal sites. Furthermore, Bader charge analysis reveals clear charge separation between protonic hydrogen and anionic oxygen, supporting the mechanistic assignment and the plausibility of the proposed reaction steps.

Among the systems studied, CoCr@gCN displays a particularly favorable energy landscape, with a highly exergonic H_2 evolution step and a modest barrier for OH* desorption. The thermodynamic driving force for hydrogen formation is reinforced by the optimized electronic structure of the Cr-Co dimer, which supports both efficient H* stabilization and manageable OH* affinity. CoMn@gCN and CoRu@gCN also exhibit favorable energetics, with both steps proceeding close to thermoneutrality, consistent with a low-energy catalytic cycle. In contrast, catalysts such as CoFe@gCN, CoNi@gCN and CoPt@gCN exhibit substantially more positive free energy barriers for OH* removal, suggesting a tendency to over-bind hydroxyl intermediates and impede catalyst turnover. The results collectively demonstrate that the HER activity on Co-M@gCN systems is governed by the energetics of OH* desorption rather than H_2 evolution, emphasizing the importance of tailoring the electronic environment to weaken OH* binding without compromising the initial water dissociation step. The dual-metal configuration enables such tuning by modulating local charge distribution and orbital overlap, highlighting the design potential of DACs for alkaline HER catalysis.

3.4. Kinetic barriers of water dissociation

Beyond the thermodynamic profiles, kinetic feasibility remains a critical descriptor for HER catalysis, especially under alkaline conditions where water dissociation constitutes the primary source of protons. To assess this, we employed the climbing image nudged elastic band (CI-NEB) method to determine the minimum energy paths and activation barriers (E_a) for the Volmer step: $H_2O^* \rightarrow H^* + OH^*$. The corresponding transition states and energy barriers for selected Co-M@gCN systems are shown in Figure 4, with quantitative values summarized in Table 2.

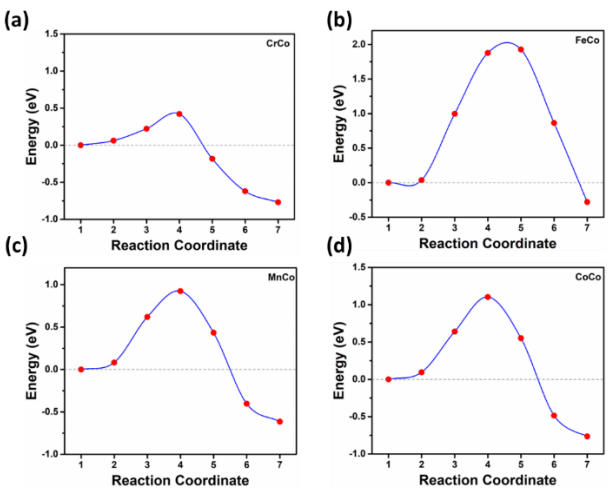

Figure 4. *Transition states (TS) and kinetic energy barriers for water dissociation ($H_2O^* \rightarrow H^* + OH^*$) on representative Co-M@gCN systems*

Among the evaluated systems, CoCr@gCN exhibits the most favorable kinetics, with an activation barrier of 0.42 eV and a moderate free energy change (ΔG_{max} = 0.49 eV). This low barrier is indicative of efficient charge redistribution and optimal orbital alignment between the Co-Cr center and the coordinated water molecule, facilitating rapid O-H bond cleavage. While CoMn@gCN shows a slightly lower ΔG_{max} (0.37 eV), its E_a rises to 0.92 eV, reflecting a higher kinetic resistance despite favorable thermodynamics. CoFe@gCN, on the other hand, demonstrates a significantly larger kinetic barrier of 1.93 eV, rendering it kinetically sluggish despite moderate ΔG values.

The trend observed among these systems highlights that thermodynamically downhill reaction steps do not guarantee facile kinetics, and vice versa. Efficient HER catalysis thus requires a balance wherein both the activation energy for water splitting and the subsequent desorption steps are within a moderate energetic window. Dual-atom configurations that enable asymmetric charge localization and orbital hybridization, such as those seen in CoCr and CoMn system, which are particularly well-suited to support such conditions.

Table 2. *Calculated maximum Gibbs free energy barrier (ΔG_{max}) and activation energy (E_a) for the water dissociation step in HER on selected Co-M@gCN systems*

Systems	CoCr@gCN	CoMn@gCN	CoFe@gCN	CoCo@gCN
ΔG_{max} (eV)	0.49	0.37	0.62	0.39
E_a (eV)	0.42	0.92	1.93	1.10

These results reinforce the notion that the Volmer step, rather than hydrogen recombination, remains the dominant kinetic bottleneck in alkaline HER on gCN-supported DACs. The ability to lower this barrier via transition metal pairing strategies provides a rational design principle for next-generation electrocatalysts.

3.5. Structure-activity relationships and electronic descriptors

To further elucidate the origin of the observed trends in HER activity, we analyzed the relationship between water adsorption behavior and local structural and electronic properties at the Co-M active sites. As shown in Figure 5a, a clear linear correlation emerges between the TM-H_2O^* bond length and the corresponding integrated crystal orbital Hamilton population (iCOHP). This relationship reflects the fundamental nature of orbital interactions: shorter bond distances result in stronger orbital overlap and hence more negative iCOHP values, indicative of covalent metal-adsorbate bonding. Among all systems, CrCo@gCN exhibits the shortest bond length and the most negative iCOHP, positioning it at the lower left of the trendline. This finding aligns with its superior catalytic kinetics, confirming that strong orbital coupling at the dual-metal site is a key enabler for water activation.

In contrast, other correlations reveal more nuanced or non-linear behavior. Figure 5b illustrates the relationship between Bader charge of the adsorbed H_2O^* species and the TM-H_2O^* bond length. Although no strict linearity is

observed, systems exhibiting smaller charge polarization within the water molecule, coupled with shorter adsorption distances, tend to exhibit more favorable reaction kinetics. This suggests that a reduced electrostatic imbalance between the H and O atoms within H_2O*, enabled by effective charge redistribution at the interface, may facilitate the cleavage of the O-H bond. This is particularly evident in systems such as CoCr, CoIr, and CoPd, where Bader charge transfer is minimal and the adsorption geometry remains compact.

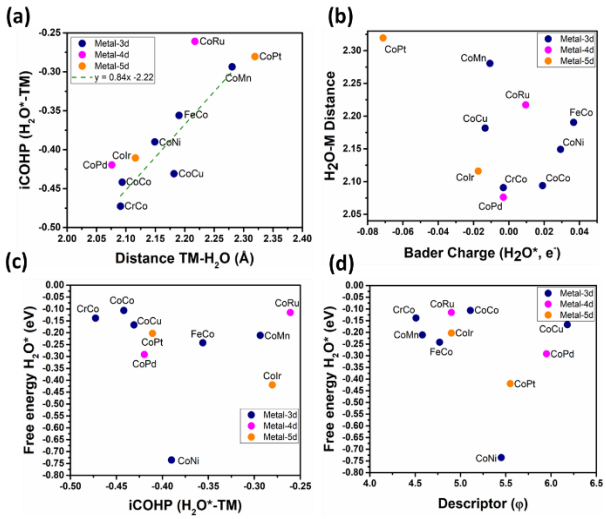

Figure 5. *Structure-activity relationships for H_2O* adsorption on Co-M@gCN systems*

(a) Linear correlation between iCOHP values and TM-H_2O bond distances, indicating stronger bonding at shorter distances. (b) Relationship between Bader charge of H_2O* and TM–H_2O* distance, reflecting charge transfer characteristics. (c) Scatter plot of iCOHP versus H_2O* adsorption free energy, showing no clear linearity and suggesting complex bonding interactions. (d) Dependence of H_2O* adsorption energy on the electronic descriptor φ, highlighting its role in reactivity trends*

A comparison between iCOHP values and the Gibbs free energy of H_2O* adsorption, shown in Figure 5c, does not yield a simple linear trend. While iCOHP captures the strength of orbital interaction between the adsorbate and the transition metal center, the overall adsorption free energy is influenced by a broader array of factors, including local strain, metal-metal coordination asymmetry, and the degree of charge delocalization across the dual-atom interface. The lack of direct proportionality underscores the complexity of adsorption phenomena on bimetallic active sites and highlights the limitations of using single-variable descriptors to predict adsorption energetics.

To bridge this complexity, we explored a composite electronic descriptor φ, defined as the ratio of the number of d-electrons (N_d) to the square root of electronegativity (E_{TM}) of the secondary metal ($\varphi = \frac{N_d}{\sqrt{E_{TM}}}$). This descriptor captures the competing effects of electron donation and charge localization, offering a compact representation of the electronic configuration at the active site. As shown in Figure 5d, although no strict linearity is observed between φ and H_2O* adsorption energy, systems with φ values in the range of 4.5-4.6, such as CrCo, and MnCo, tend to exhibit moderately strong and optimal H_2O* binding. This further supports the potential of φ as a rational screening metric for identifying catalytically competent dual-atom configurations. Taken together, these analyses reveal that HER activity on Co-M@gCN catalysts emerges from a subtle interplay of electronic interaction strength, charge transfer efficiency, and geometric compatibility between the adsorbate and dual-metal centers. A combination of short TM-H_2O* distances, strong orbital hybridization, and moderate electronic descriptors appears to be critical for enabling efficient water activation and low-barrier reaction pathways. These findings provide mechanistic insight and practical design guidelines for future development of DAC-based HER electrocatalysts.

3.6. Thermal stability from ab initio molecular dynamics simulations

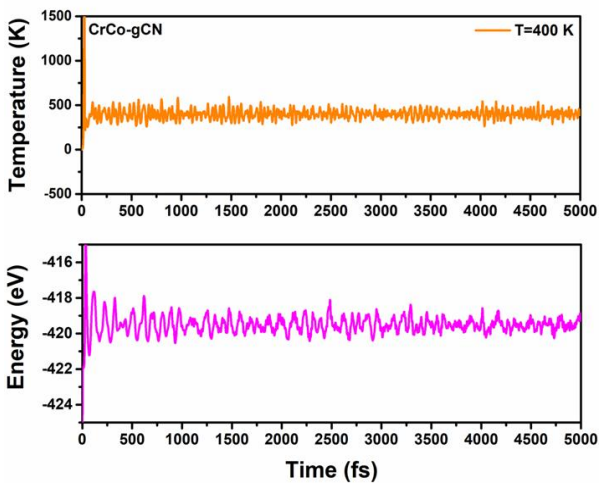

Figure 6. *Molecular dynamics simulation results at 400 K for CrCo-gCN structure over 5000 fs*

To evaluate the dynamic structural stability of the most promising catalyst, CrCo@gCN, we performed ab initio molecular dynamics (AIMD) simulations at 400 K for a total simulation time of 5 ps under the NVT ensemble. The evolution of system temperature and total energy over time is shown in Figure 6. The temperature profile remains well-centered around the target value of 400 K with only minor fluctuations, indicating effective thermostat control and thermal equilibration throughout the simulation. Concurrently, the total energy of the system exhibits moderate oscillations around an average value of approximately -420 eV, with no signs of divergence or abrupt energy spikes. This behavior confirms that the dual-metal configuration of Cr and Co on the gCN substrate is robust against thermal perturbation, with no desorption, bond breaking, or large-scale reconstruction observed during the simulation window.

These results affirm that the CoCr@gCN structure is not only thermodynamically and kinetically favorable for HER catalysis but also dynamically stable under operational conditions. The ability to maintain structural integrity at elevated temperatures further supports its viability as a practical electrocatalyst in aqueous environments.

4. Conclusion

In this work, we systematically investigated a series of Co-M dual-atom catalysts anchored on gCN for HER under alkaline conditions using density functional theory. By screening ten transition metal partners (M = Cr, Mn, Fe, Co, Ni, Cu, Pd, Ru, Ir, Pt), we assessed structural stability, electronic structure, adsorption behavior, and reaction energetics across the DAC series. Among all candidates, CoCr@gCN emerged as the most promising system, exhibiting a favorable combination of thermodynamic stability, strong orbital hybridization with H_2O*, low water dissociation barrier (E_a = 0.42 eV), optimal Gibbs free energy change for H* desorption ($\Delta G_{H^*} \approx 0.03$ eV).

Detailed analysis of spin-polarized density of states revealed that several active systems, including CoCr@gCN, exhibit half-metallic character, with asymmetric spin channels contributing to spin-selective electron transfer. Correlations between iCOHP, Bader charge, TM-H_2O* bond length, and H_2O* adsorption energy highlighted the intricate interplay between geometric and electronic factors governing HER activity. While no single descriptor fully captures all trends, a semi-empirical electronic parameter φ, constructed from the d-electron count and metal electronegativity, was found to delineate a performance window (φ ≈ 4.5-4.6) associated with optimal water adsorption and activation.

Importantly, ab initio molecular dynamics simulations confirmed that CoCr@gCN retains structural integrity at 400 K, indicating excellent thermal stability under operating conditions. Altogether, this study provides mechanistic insight into the role of dual-metal synergy, spin polarization, and metal-support interaction in promoting HER activity, and establishes CoCr@gCN as a high-performing and robust DAC for alkaline hydrogen production. The design principles outlined herein offer a transferable framework for guiding future discovery and rational optimization of low-cost, earth-abundant DACs for energy conversion applications.

Acknowledgements: This research was financially supported by the Vietnam Ministry of Education and Training, Vietnam (code: B2023.DNA.08).

REFERENCE

[1] J. A. Turner, "Sustainable hydrogen production", *Science*, vol. 305, no. 5686, pp. 972-974, 2004.

[2] Z. W. Seh, J. Kibsgaard, C. F. Dickens, I. Chorkendorff, J. K. Nørskov, and T. F. Jaramillo, "Combining theory and experiment in electrocatalysis: Insights into materials design", *Science*, vol. 355, no. 6321, p. eaad4998, 2017.

[3] X. Zou and Y. Zhang, "Noble metal-free hydrogen evolution catalysts for water splitting", *Chemical Society Reviews*, vol. 44, pp. 5148-5180, 2015.

[4] B. Qiao *et al.*, "Single-atom catalysis of CO oxidation using Pt1/FeOx", *Nature Chemistry*, vol. 3, no. 8, pp. 634-641, 2011.

[5] J. Liu, "Catalysis by supported single metal atoms", *ACS Catalysis*, vol. 7, no. 1, pp. 34-59, 2017.

[6] X. F. Yang, A. Wang, B. Qiao, J. Li, J. Liu, and T. Zhang, "Single-atom catalysts: A new frontier in heterogeneous catalysis", *Accounts of Chemical Research*, vol. 46, no. 8, pp. 1740-1748, 2013.

[7] X. Li, X. Yang, J. Zhang, Y. Huang, T. Zhang and J. Liu, "Single-atom catalysts for electrochemical hydrogen evolution reaction: Recent advances and future perspectives", *Advanced Materials*, vol. 33, no. 20, p. 2004359, 2021.

[8] A. Wang, J. Li, and T. Zhang, "Heterogeneous single-atom catalysis", *Nature Reviews Chemistry*, vol. 2, no. 6, pp. 65-81, 2018.

[9] L. Zhang, L. Han, H. Liu, X. Liu, and J. Luo, "Atomically dispersed Co-N-C catalyst with hierarchical porosity for efficient and stable hydrogen evolution", *Advanced Energy Materials*, vol. 9, no. 14, p. 1803572, 2019.

[10] H. Li, X. Wang, and S. Dai, "Single-atom and dual-atom catalysts for electrochemical energy conversion", *Chemical Society Reviews*, vol. 49, no. 20, pp. 7356-7413, 2020.

[11] Z. Zhang, H. Zhao, Y. Zhou, X. Tian, Y. Liu and X. Duan, "Synergistic effects in dual-atom catalysts for electrochemical energy conversion", *Advanced Materials,* vol. 34, no. 11, p. 2106060, 2022.

[12] A. Kumar *et al.*, "Moving beyond bimetallic-alloy to single-atom dimer atomic-interface for all-pH hydrogen evolution", *Nature Communications*, vol. 12, p. 6766, 2021.

[13] Huong T. D. Bui *et al.*, "Activity-Selectivity Enhancement and Catalytic Trend of CO2 Electroreduction on Metallic Dimers Supported by N-Doped Graphene: A Computational Study", *J. Phys. Chem*. C, vol. 125, no. 24, pp. 13176-13184, 2021.

[14] H. T. D. Bui *et al.*, "DFT insights into dual-site synergy of Ni-Fe on defective graphene for enhanced HER performance", *Physical Chemistry Chemical Physics*, vol. 23, pp. 25143-25151, 2021.

[15] Y. Wang, Q. Li, Y. Bi, Y. Wu, X. Zhang, and Y. Sun, "Recent advances in dual-atom catalysts for energy-related electrocatalysis", *Small*, vol. 19, no. 16, p. 2207282, 2023.

[16] Y. Wang, X. Wang, and M. Antonietti, "Polymeric graphitic carbon nitride as a heterogeneous organocatalyst: from photochemistry to multipurpose catalysis to sustainable chemistry", *Angewandte Chemie International Edition*, vol. 51, no. 1, pp. 68-89, 2012.

[17] J. Zhang, Y. Chen, and X. Wang, "Two-dimensional covalent carbon nitride nanosheets: synthesis, functionalization, and applications", *Energy & Environmental Science,* vol. 8, no. 11, pp. 3092-3108, 2015.

[18] X. Liu *et al.*, "Advanced dual-atom catalysts on graphitic carbon nitride for enhanced hydrogen evolution via water splitting", *Nanoscale*, vol. 16, pp. 13148-13159, 2024.

[19] Y. He, F. Chen, and G. Zhou, "Graphitic carbon nitride supported Ni-Co dual atom catalysts beyond Ni1(Co1) single atom catalysts for hydrogen production: A density functional theory study", *Phys. Chem. Chem. Phys*., vol. 26, pp. 14364-14373, 2024.

[20] X. Lu, L. Xu, I. Ullah, H. Li, and A. Xu, "Sulfur-doped g C3N4 photocatalyst for significantly steered visible light photocatalytic H2 evolution from water splitting", *Catal. Sci. Technol*., vol. 14, pp. 606-614, 2024.

[21] M. Makaremi, S. Grixti, K. T. Butler, G. A. Ozin, and C. V. Singh, "Band Engineering of Carbon Nitride Monolayers by N-Type, P-Type, and Isoelectronic Doping for Photocatalytic Applications", *ACS Appl. Mater. Interfaces*, vol. 10, no. 13, pp. 11143-11151, 2018.